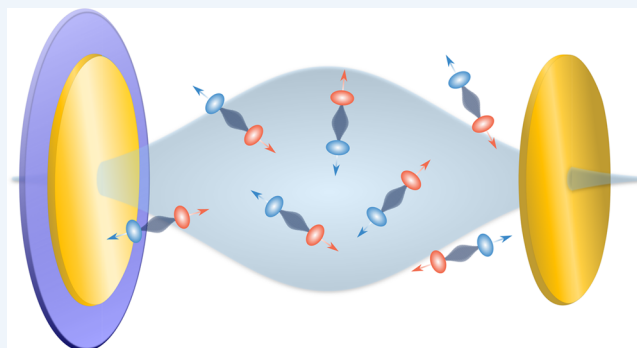


Hybrid Light–Matter States in a Molecular and Material Science Perspective

Thomas W. Ebbesen*

ISIS and USIAS, University of Strasbourg and CNRS, 8 allée Monge, 67000 Strasbourg, France

CONSPECTUS: The notion that light and matter states can be hybridized the way s and p orbitals are mixed is a concept that is not familiar to most chemists and material scientists. Yet it has much potential for molecular and material sciences that is just beginning to be explored. For instance, it has already been demonstrated that the rate and yield of chemical reactions can be modified and that the conductivity of organic semiconductors and nonradiative energy transfer can be enhanced through the hybridization of electronic transitions. The hybridization is not limited to electronic transitions; it can be applied for instance to vibrational transitions to selectively perturb a given bond, opening new possibilities to change the chemical reactivity landscape and to use it as a tool in (bio)molecular science and spectroscopy. Such results are not only the consequence of the new eigenstates and energies generated by the hybridization. The hybrid light–matter states also have unusual properties: they can be delocalized over a very large number of molecules (up to ca. 10^5), and they become dispersive or momentum-sensitive. Importantly, the hybridization occurs even in the absence of light because it is the zero-point energies of the molecular and optical transitions that generate the new light–matter states. The present work is not a review but rather an Account from the author's point of view that first introduces the reader to the underlying concepts and details of the features of hybrid light–matter states. It is shown that light–matter hybridization is quite easy to achieve: all that is needed is to place molecules or a material in a resonant optical cavity (e.g., between two parallel mirrors) under the right conditions. For vibrational strong coupling, microfluidic IR cells can be used to study the consequences for chemistry in the liquid phase. Examples of modified properties are given to demonstrate the full potential for the molecular and material sciences. Finally an outlook of future directions for this emerging subject is given.



■ INTRODUCTION

Perhaps the easiest way to understand the formation of hybrid light–matter states is to start with an all-molecular analogy, namely, the formation J- and H-aggregates, where the molecular transition moments of the aligned molecules couple to give rise to two new eigenstates, as illustrated in Figure 1a.¹ The fluctuating transition dipole moments generate the interaction just in the same way that fluctuating ground-state dipole moments contribute to van der Waals forces. If one places molecules for instance inside an optical cavity, as illustrated in Figure 2a, that is tuned to a given molecular transition, then Figure 1a can be replaced by Figure 1b, where one side is now replaced by the optical mode of the cavity. In this quantum electrodynamics (QED) picture, the optical cavity is just another oscillator with its own zero-point energy.² The new hybrid states thus formed, known as polaritonic states, have the following wave functions:

$$|P^+\rangle = c_{11}|e\rangle_m|0\rangle_c + c_{12}|g\rangle_m|1\rangle_c \quad (1)$$

$$|P^-\rangle = c_{22}|e\rangle_m|0\rangle_c + c_{21}|g\rangle_m|1\rangle_c \quad (2)$$

where P^+ and P^- are constructed as linear combinations of the molecule in the excited state (e) with 0 photons in the cavity and the molecule in the ground state (g) with 1 photon in the

cavity. The phenomenon leading to the formation of P^+ and P^- is known in physics as light–matter strong coupling. The P^+ and P^- wave functions are hybrids in the true sense since they are combinations of components with different spins, the Fermionic electronic part and the bosonic photonic part. P^+ and P^- are separated by what is known as the Rabi splitting energy (Figure 1b). Figure 2b illustrates what happens to the absorption spectrum of molecules when they are placed in a cavity that is resonant with the molecular transition and the conditions are right for the hybridization.

Historically, light–matter strong coupling was mainly the province of physicists, working first with atoms and then with semiconductors.^{2–5} The quasi-bosonic nature of the polaritons generated for instance by exciting a transition to P^- and P^+ has been the focus of much interest, as it has led to the promises of low-threshold lasers, photoluminescent devices, and high-temperature Bose–Einstein-like condensation of polaritons.^{3,4} The coupling of phonon modes to surface plasmon resonances^{6,7} was followed by the first demonstration of light–molecule strong coupling in 1982.⁸ However, it was not until two papers^{9,10} appeared in 1998 that light–molecule

Received: June 22, 2016

Published: October 25, 2016



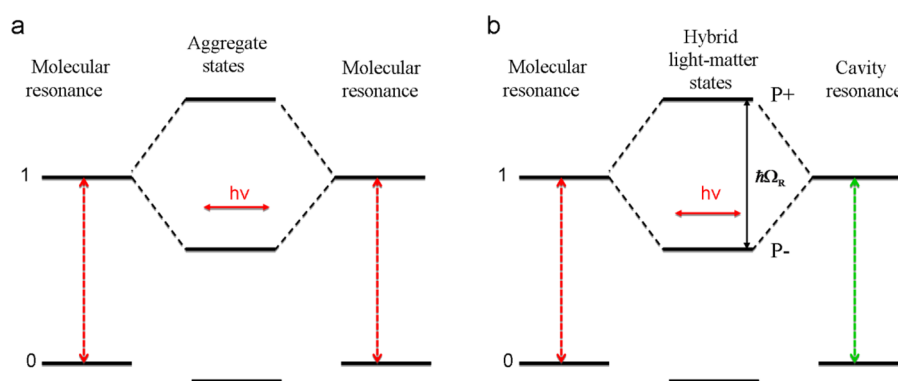


Figure 1. Schematic diagrams of (a) the all-electronic coupling between transition dipole moments leading to the formation of J- and H-aggregates with their new energy levels and (b) the similar process between a molecular transition and a cavity resonance, in which the two hybrid light–matter states $P+$ and $P-$ are separated by the so-called Rabi splitting energy $\hbar\Omega_R$.

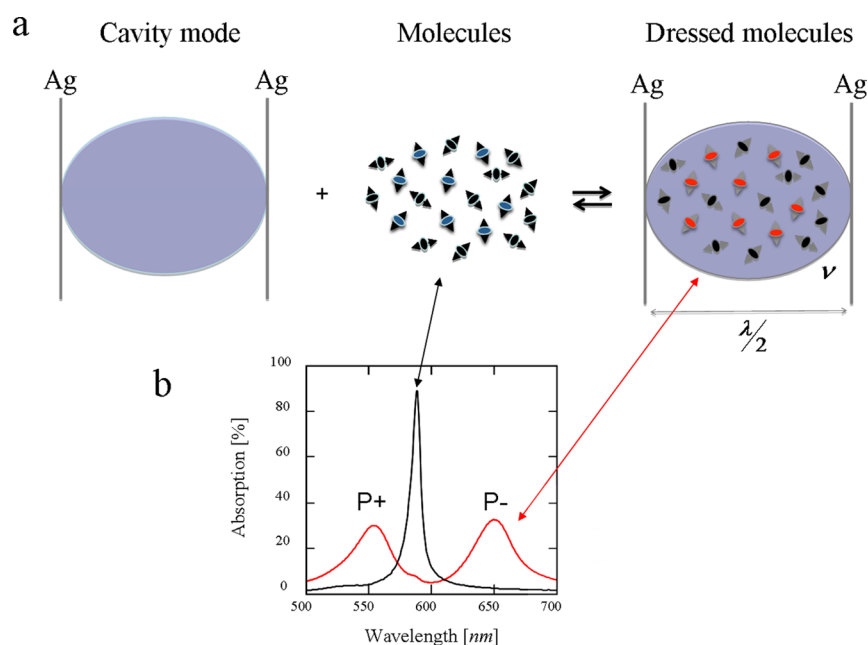


Figure 2. (a) Schematic diagram of the $\lambda/2$ mode formed between two Ag mirrors (a Fabry–Perot cavity) that is resonant with the absorption of molecules (shown as little dipoles), which, when placed inside the cavity, interact strongly with the mode, resulting in the formation of light–matter hybrid states. The molecules are said to be dressed by the electromagnetic field. (b) Experimental absorption spectrum of a cyanine dye molecule before (black curve) and after (red curve) undergoing light–matter strong coupling with a cavity. Reproduced in part from ref 27.

strong coupling generated increased interest among physicists, leading eventually to the observation of lasing and polariton condensation at room temperature in 2014.^{11–13}

What stimulated our curiosity when we started working on this topic¹⁴ was the impact of light–matter hybridization on typical molecular and material properties, something that had not at all been investigated.^{15–30} Therefore, the focus here is first on the properties of the hybrid states and then on their resulting impact on well-known properties such as conductivity and chemical reactivity, presented from the perspectives of both molecular and materials sciences. To better address these issues, it is necessary to recall some of the underlying physics.

■ UNDERLYING PHYSICS

The physics of light–matter interactions are typically classified as being in either the weak or strong coupling regime.² In the weak coupling regime, the radiative properties of the atom or molecule are modified. The best example of this is the Purcell effect, whereby the radiative rate constant and emission

quantum yield of an excited state are changed by for instance placing the molecules in the confined electromagnetic field of a resonant cavity. In the strong coupling regime, hybrid light–matter states are formed, as described in the previous paragraphs, whenever the two resonant components exchange energy faster than any decay process. This is a key condition for achieving strong coupling and can be seen immediately in the Jaynes–Cummings two-state model that relates the Rabi splitting to a number of variables, including dissipation:^{5,31,32}

$$\Delta E = E_+ - E_- = \hbar\Omega_R = \sqrt{4V_n^2 - (\Gamma_c - \Gamma_e)^2} \quad (3)$$

where E_+ and E_- are the energies of $P+$ and $P-$, respectively, Γ_c and Γ_e are given by the decay constants ($\Gamma = \hbar/\tau$) of the photon in the cavity and the excited state, respectively, and V is the interaction energy between the electric component of the electromagnetic field in the cavity, E_0 , and the transition dipole moment of the material, d . In the absence of dissipation, the Rabi splitting is simply

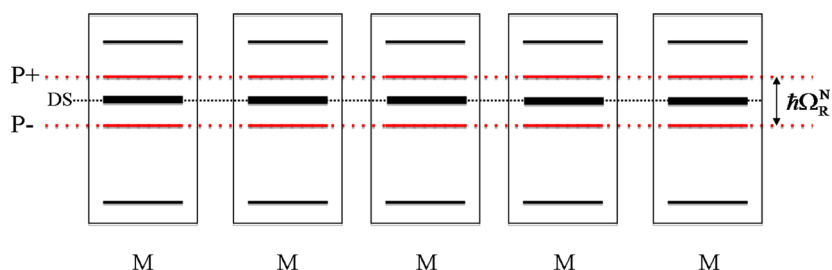


Figure 3. Illustration of the collective states (P+, P–, and dark states (DS)) delocalized over many molecules M.

$$\hbar\Omega_R = 2V_n = 2\mathbf{d} \cdot \mathbf{E}_0 = 2d \sqrt{\frac{\hbar\omega}{2\epsilon_0 v}} \times \sqrt{n_{\text{ph}} + 1} \quad (4)$$

where $\hbar\omega$ is the resonant energy, ϵ_0 is the vacuum permittivity, v is the volume of the electromagnetic mode (Figure 2), and n_{ph} is the number of photons involved in the coupling process. From the last factor in eq 4, it is immediately clear that even in the absence of photons $\hbar\Omega_R$ has a residual value known as the vacuum Rabi splitting. The word “vacuum” here refers to the vacuum (electromagnetic) field in the cavity (i.e., the zero-point energy of the cavity) and not to the absence of matter. In all that follows, we will always be in this limit, as we will consider systems where many molecules are coupled to a single mode and where adding photons does not increase $\hbar\Omega_R$. From a QED point of view, the zero-point-energy interaction between the cavity and molecular transitions is due to the exchange of virtual photons (Figure 1).

The volume v of an electromagnetic mode of a microcavity or a surface plasmon is typically very large ($\sim\lambda^3$ or $\sim\mu\text{m}^3$ in the visible) compared with the volume occupied by a molecule ($\sim\text{nm}^3$), so it is possible for the number of molecules within one mode and interacting with it, N , to be very large (Figure 2), which results in a significant enhancement of the Rabi splitting since $\hbar\Omega_R \propto \sqrt{N/v}$. Considering the molecular density, strong coupling in the visible spectrum can involve as many as $\sim 10^5$ molecules, resulting in vacuum Rabi splittings on the order of 1 eV. To observe such large splittings, the other parameters in eq 4 must also be optimized: the transition dipole moment (i.e., the molar absorption coefficient) should be as high as possible, and the mode volume should be minimal to maximize E_0 . The latter is obtained by using metallic mirrors for a standard Fabry–Perot (FP) cavity or plasmonic structures,³³ which concentrate the field at the metal surface. Cavities made from dielectric mirrors can give rise to much sharper transmission resonances, but this comes at the expense of larger mode volumes as a consequence of the multiple reflections on the different dielectric layers composing the mirrors.

The experimental realization of hybrid light–matter states through strong coupling is quite straightforward. The simplest is the use of an FP cavity. A glass slide is coated with a thin metallic film (e.g., 30 nm of Ag). A polymer heavily loaded with the dye (typically 50% by weight) is then spin-coated on top of the mirror to the desired thickness so that when a second mirror is deposited on top, the cavity is in resonance with the absorption peak to be coupled. Figure 2b shows an example of the consequences of strong coupling on the absorption spectrum of the sample, with the appearance of two new absorption peaks corresponding to the transitions to P+ and P–. The energy separation between the two peaks reflects not just the Rabi splitting but also the rate of energy exchange

between the molecules and the optical mode, ν_R , since this quantity is given by

$$\nu_R = \frac{\hbar\Omega_R}{h} = \frac{\Omega_R}{2\pi} \quad (5)$$

ν_R must be higher than the rates of decay of the constituent states, namely, the excited state and the photon in the cavity. The latter can be calculated from the full width at half-maximum (FWHM) of the optical mode ($\tau = \hbar/\Gamma_{\text{FWHM}}$). In other words, the two new hybrid peaks must be separated by more than the FWHM of both the molecular absorption and the optical mode. The shape of the polaritonic absorption peaks is mostly determined by the spectral features of the cavity mode.

It should be noted that judging whether strong coupling has been attained from the appearance of two transmission peaks for the coupled system can be very misleading.³¹ After all, any absorber can split a transmission peak in two. Therefore, both the reflection (R) and transmission (T) must be measured to calculate the absorption (A) spectrum ($A = 1 - T - R$). Another important check is to measure the dependence of the Rabi splitting on the concentration (C), i.e., $\hbar\Omega_R \propto \sqrt{N/v} = \sqrt{C}$. Other features such as the angular dependence will be discussed in the next section.

FUNDAMENTAL PROPERTIES OF HYBRID LIGHT–MATTER STATES

Collective States

As already discussed, the strong coupling of a large number of molecules to a given optical mode significantly enhances $\hbar\Omega_R$. The large splitting perturbs the levels of the other molecular eigenstates that are not directly involved in the coupling, as illustrated in Figure 3. It also implies that the N molecules generate $N + 1$ collective states, of which two are detectable (P+ and P–) and the other $N - 1$ linear combinations are collective dark states (so-called because transitions to these states from the ground state are forbidden).³¹ The important point is that the wave function of these hybrid states can be delocalized over ca. 10^N molecules in the mode volume, offering a unique possibility to affect the electronic and energy transport in molecular systems, as will be seen. Moreover, it has been shown that the emission from P– is spatially coherent over micrometer distances, resulting in interference fringes.^{34,35} In other words, coupled molecules that are micrometers apart emit in-phase!

It has been argued that the Rabi splitting experienced by each molecule involved in the collective coupling is not $\hbar\Omega_R$ but $\hbar\Omega_R/\sqrt{N}$. If this were the case, the splitting would be tiny, and it is unlikely that any molecular or material property would be modified as observed experimentally. As discussed below, the

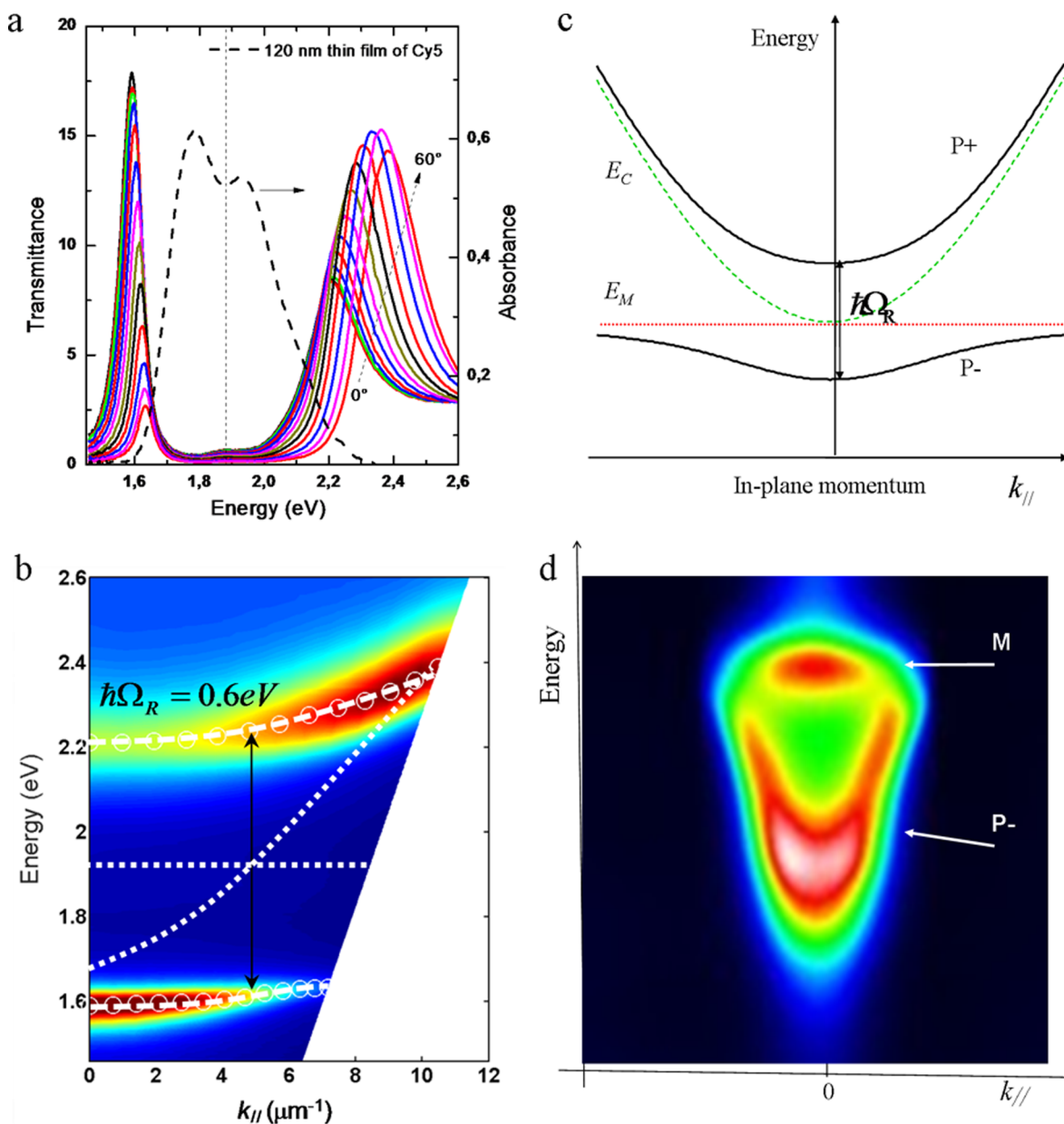


Figure 4. (a) Absorption spectrum of a thin film of carbocyanine dye (Cy5) and the corresponding transmission spectra of a strongly coupled system measured as a function of angle (every 5°). (b) Replot of the data in (a) as a dispersion curve. A gap (anticrossing) appears at the intersection of the nondispersive Cy5 absorption peak and the dispersive optical mode of the FP cavity, from which the Rabi splitting can be determined. (c) Illustration of an FP cavity tuned such that the anticrossing appears at normal incidence ($k_{||} = 0$). E_C is the FP cavity resonance (dashed green line), and E_M is the molecular transition energy (dotted red line). (d) Emission of a strongly coupled dye molecule plotted as a function of $k_{||}$ according to eq 6. The nondispersive emission (M) is from the uncoupled molecules in the cavity, while the coupled ones give rise to dispersive emission from $P-$.

chemical reactivity of individual molecules is directly affected by the collective coupling strength,^{16,30} as theoretical studies have recently confirmed.³⁶

Angular Dispersion

Another particular behavior of hybrid light–matter states is that they inherit the dispersive behavior of the photonic component (see ref 37 for an introduction to dispersion curves). In other words, their properties become dependent on momentum and therefore on angle, as illustrated in Figure 4a for the spectrum of cyanine dye coupled to a cavity mode. Physicists conveniently replot such data as energy versus the in-plane momentum $k_{||}$ to visualize the dispersive nature of the hybrid

states (as illustrated in Figure 4b). For an FP cavity, the following formula can be used to plot such dispersive curves:

$$|k_{||}| = k_{||} = \frac{2\pi}{\lambda} \sin \theta \quad (6)$$

where θ is the angle of incidence and λ is the peak wavelength. The intersection of the nondispersive dye absorption band and the dispersive optical component leads to an anticrossing (Figure 4b). It is important to note that an anticrossing alone is not proof of strong coupling. The Rabi splitting is defined by this *minimum* energy gap, where the photonic and material components are isoenergetic and contribute equally to the

hybrid states. At larger k_{\parallel} values, P+ has an increasing photonic component while P− becomes more material-like (Figure 4b). Figure 4c illustrates the shape of the dispersion when the absorber is at resonance with the optical mode at normal incidence ($k_{\parallel} = 0$), and Figure 4d shows a corresponding experimental result for the emission of P− plotted in the same way according to eq 6. This implies that if one wishes to determine for instance the P− emission quantum yield, it must be integrated over all angles. Figure 4d also shows some nondispersive fluorescence from uncoupled molecules as discussed next.

Field Strength, Molecular Orientation, and Fraction of Coupled Molecules

From eq 4, the Rabi splitting is expected to be strongly dependent on the field strength E_0 . This can be seen by varying the position of a thin molecular layer of 5,6-dichloro-2-[[5,6-dichloro-1-ethyl-3-(4-sulfobutyl)benzimidazol-2-ylidene]-propenyl]-1-ethyl-3-(4-sulfobutyl)benzimidazolium hydroxide sodium salt (TDBC) J-aggregates inside an FP cavity that is resonant with the molecules (Figure 5a). The vacuum field is

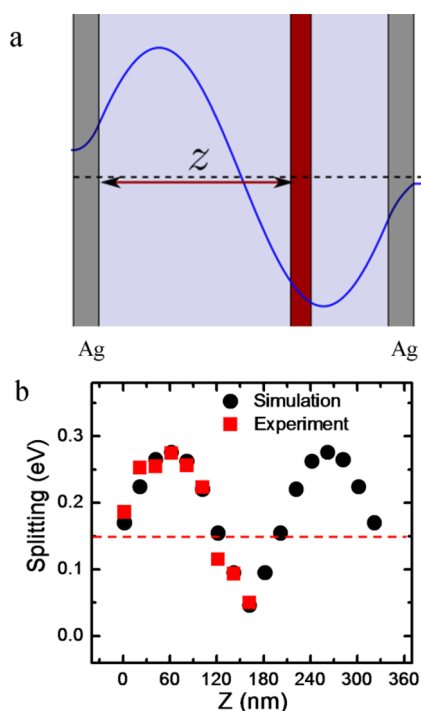


Figure 5. (a) A 20 nm layer of TDBC J-aggregates is placed at different positions (z) between the two Ag mirrors of a resonant FP cavity. The molecules interact with different electric field strengths (blue line), and as a consequence, the Rabi splitting varies with z as shown in (b). The red dashed line is the minimum splitting above which the strong coupling condition of eq 5 is met. Reprinted from ref 20. Copyright 2014 American Chemical Society.

not constant in the cavity, approaching 0 at the nodes and a maximum at the antinodes. The value of $\hbar\Omega_R$ follows the field strength precisely (Figure 5b), so the Rabi splitting is maximized by placing a given number of molecules in the vicinity of the antinode compared with having them spread evenly throughout the cavity.²⁰

The coupling strength is also sensitive to the relative orientation of the molecular transition dipole moments \mathbf{d} and \mathbf{E}_0 . In an FP cavity, the maximum interactions would be in a

plane parallel to the mirrors, while the molecules whose transition dipole moments are perpendicular to this plane would not couple to the cavity. Therefore, in typical samples with random molecular orientations in a varying electric field, the measured $\hbar\Omega_R$ is an *average* value. As a consequence, when one measures a given property for a coupled system, it is composed of the sum of the uncoupled and coupled molecules, e.g., as illustrated with the emission shown in Figure 4d. The ratio of coupled to uncoupled molecules has been treated as the consequence of the thermodynamics of the coupling process.²¹

Polariton Lifetimes and Emission Quantum Yield

At first thought, once P+ and P− are populated, their lifetimes should not be much longer than the shortest lifetime of the molecular and optical components from which they are constructed. This is the lifetime of the photon in a metallic cavity or a plasmon mode, which is typically less than 50 fs. However, nature is full of examples to the contrary, such as molecular excimers and exciplexes, which can be much longer lived than the excited states from which they are formed.

In the case of the experimental observations of P− and P+ lifetimes, the interpretation depends very much on the groups involved, and this might be due to the fact that the results are sensitive to the coupling strength.³⁸ Some see in the very short spectral relaxation times (below 100 fs) the fact that the lifetimes of both P+ and P− are indeed limited by the optical component (see, e.g., ref 39). However, at very high coupling strength, we find that while P+ is very short lived (<150 fs) like typical upper excited states because of nonradiative decay channels, the P− lifetime is comparable to or sometimes even longer than that of the molecular component, on the picosecond time scale. This is observed from both the transient absorption and the emission lifetime of P−. For instance, in the case of thin layers of J-aggregates deposited at a specific location inside an FP cavity (Figure 5), the decay of P− is complete within a few picoseconds, and the measured half-lives are collected in Table 1 and compared with that of the

Table 1. Comparison of the Properties of the Excited State J_1 of the TDBC J-Aggregate Outside the Cavity (Bare Film) and Inside the Cavity at the Node (Zero-Field) with Those of P− Formed by Placing the TDBC at the Antinode (Maximum Field)^a

	J_1 of bare film	J_1 of λ cavity node	P− of λ cavity antinode
$\tau_{1/2}$ (ps)	0.6	0.6	1.4
Φ_E	2×10^{-2}	1×10^{-3}	1×10^{-2}
k_r (s^{-1})	3×10^{10}	1.7×10^9	7.1×10^9
k_{nr} (s^{-1})	1.6×10^{12}	1.7×10^{12}	7.1×10^{11}

^aAs shown in Figure 4, at the antinode the strong coupling leads to the highest value of $\hbar\Omega_R$.²⁰

uncoupled sample. As can be seen, $\tau_{1/2}^{P-}$ is more than twice that of the bare J-aggregate and 1000 times longer than the lifetime of the photon in the cavity. One way to check whether this is reasonable is to measure the emission quantum yield of P−, since this quantity is given by

$$\Phi_E^{P-} = \frac{k_r^{P-}}{k_r^{P-} + k_{nr}^{P-}} = k_r^{P-} \tau^{P-} \approx k_r^{P-} \tau_{1/2}^{P-} \quad (7)$$

and k_r^{P-} can be calculated from the absorption peak of P− using the Bowen–Wokes formula.²⁰ The value of $\tau_{1/2}^{P-}$ determined from Φ_E^{P-}/k_r^{P-} is within a factor of 2 of the experimental value

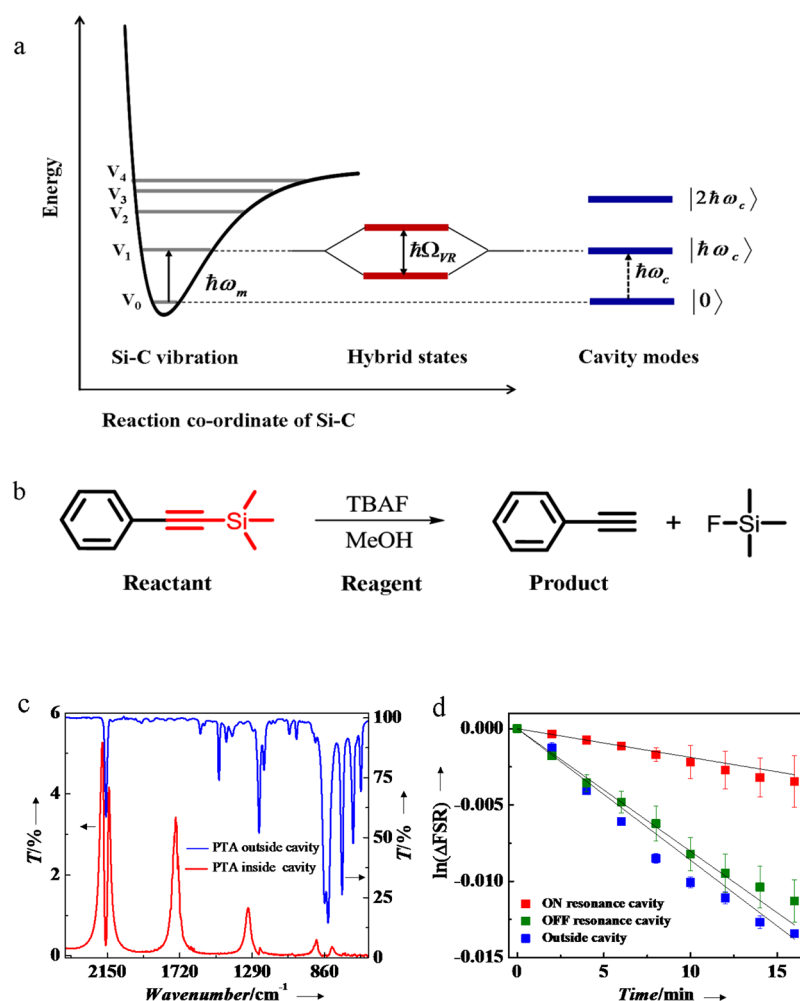


Figure 6. (a) Schematic illustration of the light–matter strong coupling between the Si–C stretching vibrational transition and a cavity mode resulting in the Rabi splitting. (b) The silane deprotection reaction of 1-phenyl-2-trimethylsilylacetylene (PTA) with tetra-*n*-butylammonium fluoride (TBAF). (c) IR transmission spectrum of PTA before (blue trace) and after (red trace) it was placed inside an FP cavity having a series of resonances, one of which was strongly coupled to the C–Si stretching modes at 860 cm⁻¹. (d) Kinetics of the reaction extracted from the temporal shifts in the higher-order cavity modes in an on-resonance cavity (red squares), outside the cavity (blue squares), and in an off-resonance cavity (green squares). Reprinted from ref 30.

directly measured by pump–probe spectroscopy. In other words, the emission quantum yield is only compatible with a long P– lifetime.²⁰ With an emission quantum yield on the order of 10⁻², the P– lifetime in the above example is dominated by the nonradiative events such internal vibrational relaxation and intermolecular dissipation of the excitation energy.

The above findings are also consistent with systems with large Rabi splittings that are in the non-Markovian regime, where the dynamics of the coupled state cannot be estimated from that of the uncoupled constituents, and hence, the lifetime of the coupled state can be longer than that of either uncoupled state.²²

■ MOLECULAR AND MATERIAL PROPERTIES UNDER STRONG COUPLING

While molecules have been mostly studied under strong coupling to an electronic transition (ESC), vibrational strong coupling (VSC) also has much potential (refs 38–58 provide a sampling of recent studies by other groups). Below a few examples of modified properties taken from our work are given.

Coupling of a Chemical Reaction to the Vacuum Field

The splitting of the excited state by ESC naturally modifies the internal dynamics of the excited states (as discussed above) and the excited-state potential surface. This has immediate consequences for the excited-state reactivity, as we demonstrated for the first time with a photoisomerization reaction and then confirmed theoretically with stilbene as a model compound.³⁶ As we concluded at the time, it should also be possible to modify ground-state chemistry by VSC.¹⁶ After all, by strong coupling to a given vibration, as illustrated in Figure 6a, the vibrational frequency ω_v is lowered by the splitting, and thus the bond strength f might be weakened, since

$$\omega_v \propto \sqrt{\frac{f}{\mu}}$$

where μ is the reduced mass of the atoms involved in the vibration. In addition, the Morse potential should then be modified. Technically, samples can be strongly coupled in microfluidic IR FP cells,^{26,52} and the reactions can be monitored in the liquid phase. A first example of the effect of VSC on chemical reactivity was recently reported.³⁰ We chose

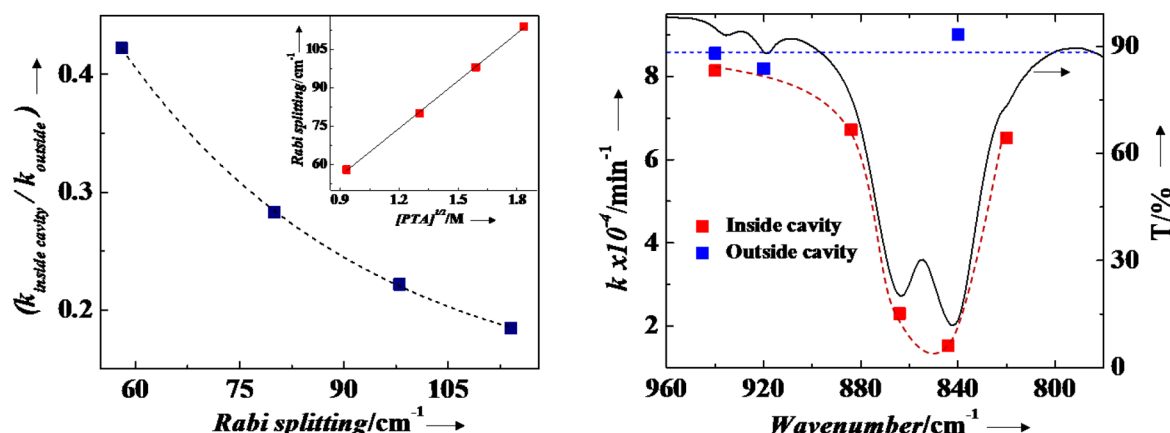


Figure 7. (a) Plot showing the reduction in the ratio of the reaction rate under VSC to that outside the cavity as a function of the Rabi splitting energy. The inset shows the linear dependence of the Rabi splitting on the square root of [PTA]. (b) Plot showing the reaction rates inside (red squares) and outside (blue squares) the cavity as functions of the cavity tuning. The black solid line shows the double-peaked IR absorption peak associated with the Si–C modes of PTA. The dotted lines are guides to the eye. Reprinted from ref 30.

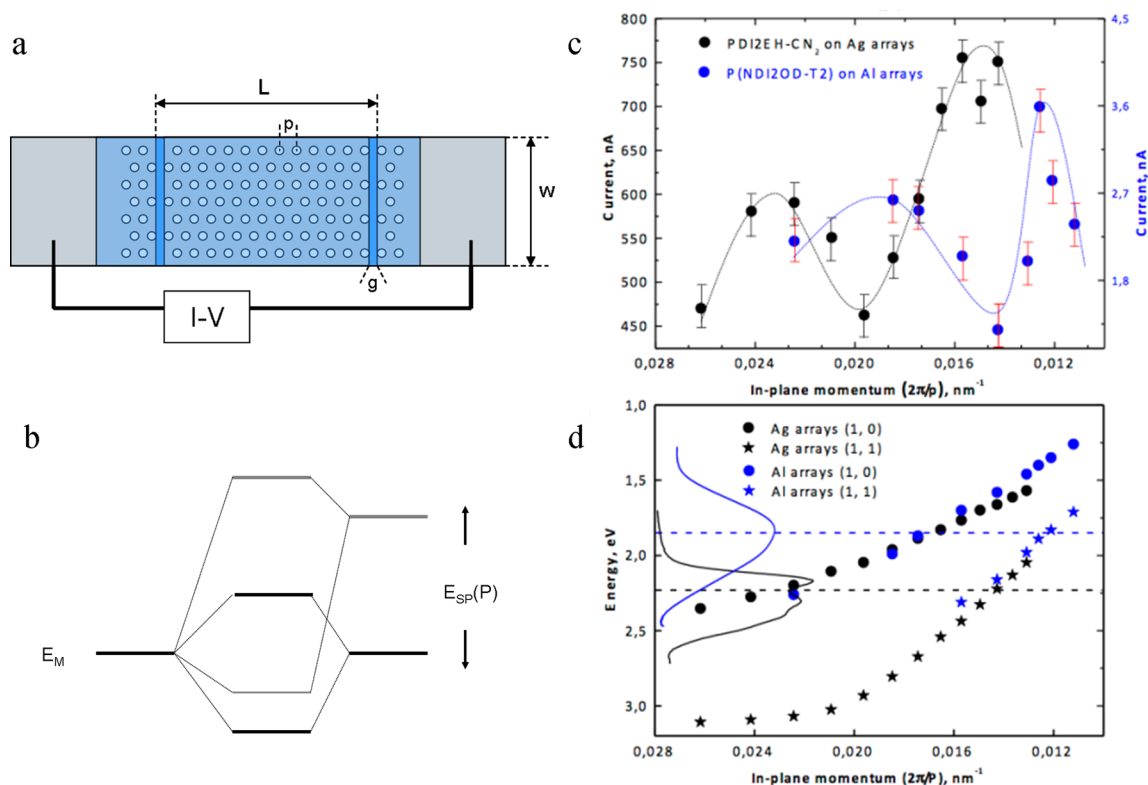


Figure 8. (a) Schematic diagram of the setup for measuring the I – V curves of organic semiconductors interacting with plasmonic modes of a hole array between a source and a drain. (b) The energy of the plasmonic modes (E_{SP}) of the hole array was varied by changing the period P of the holes so that it crosses the transition energy of the organic semiconductor (E_M). (c) Plot of the current at a given voltage as a function of $k_{||} = 2\pi/P$, revealing two current peaks for two different semiconductors. (d) The current peaks correspond exactly to where the nondispersive absorptions of the semiconductors (dashed lines) cross two of the plasmonic modes. At these crossings, strong coupling occurs with a Rabi splitting of ~ 0.7 eV. Reproduced from ref 28.

the pseudo-first-order deprotection reaction of an alkynyl silane (Figure 6b). The cavity was tuned to be resonant with the stretching transitions of the C–Si bonds around 860 cm^{-1} , a double peak corresponding to the $\equiv\text{C}$ –Si and $-\text{Si}-$ modes. The reaction slowed by a factor of 5.5 under VSC (Figure 6d). The change in reaction rate under VSC was very sensitive to the collective Rabi splitting $\hbar\Omega_R$ (Figure 7a) and the tuning of the IR cavity resonance to the vibrational band (Figure 7b).

Qualitative GC–MS analysis of the progress of the reaction also confirmed the decrease in the reaction rate.³⁰ Temperature studies for a given Rabi splitting showed that the enthalpy of activation ΔH^\ddagger increased from 39 to 96 kJ mol^{-1} under VSC, while the entropy of activation ΔS^\ddagger went from -171 to $7.4\text{ J K}^{-1}\text{ mol}^{-1}$, suggesting a change from an associative to a dissociative transition state.

Such remarkable changes in reaction rates and thermodynamics clearly indicate that the reactivity landscape is

significantly modified with many consequences, as discussed below.

Coupling of Materials to the Vacuum Field

Under ESC, the Rabi splitting can be as large as around 1 eV, corresponding to a significant fraction of the original transition energy. This is known as the ultrastrong coupling regime, where the other eigenstates of the material are also significantly perturbed, leading to modification of the ground-state properties and, more generally speaking, of the bulk material properties. Indeed, we have found changes in the work function of an organic material and in the phase transition of a perovskite under strong coupling.^{17,19}

Transport properties of materials should benefit from the delocalized nature of hybrid light–matter states. To test this possibility, three different organic semiconductors known to have very different mobilities were placed on plasmonic structures (hole arrays) whose resonances could be tuned by varying the period P .²⁸ At resonance the Rabi splitting was about 0.7 eV for all three compounds. The current–voltage curves were recorded as a function of P , and when the current for a given voltage was plotted as a function of k ($=2\pi/P$), two peaks in the current appeared, corresponding to strong coupling with two different plasmonic resonances of the array, as shown in Figure 8. When the absorption peak of the organic material shifted, the current resonances occurred at the new crossings with the plasmonic modes. The increase in conductivity reflects a corresponding change in charge mobility, and for the best semiconductor it was enhanced by an order of magnitude under strong coupling. A theoretical model shows that delocalized states play a key role, including not only P – but more importantly the dark states (Figure 3), which have much higher density.²⁸

The above experimental results also stimulated theoretical studies of energy (or polariton) transport via the polaritonic states, which should be extremely efficient again due to their delocalization.^{55,56} The analogous donor (D) to acceptor (A) energy transfer has been investigated under ESC. In one study,⁵⁷ energy transfer was reported on the basis of excitation spectra, but no change in lifetime of the donor was found as would have been expected for nonradiative energy transfer. We found that the Förster-type nonradiative transfer rate can be increased by a factor of 7 with an efficiency approaching unity.²⁹ Thus, strong coupling can be used not only to modify the spectral response of absorbers but also to direct energy efficiently to a given molecule or detector. Metal-to-semiconductor electron transfer has also been boosted by ESC,⁵⁰ and theoretical simulations predict up to a 3 orders of magnitude increase in electron transfer reaction rates.⁴⁸

OUTLOOK

The modifications induced by strong coupling can be found in the bulk properties as well as at the level of molecules. The collective states generated by strong coupling offer unique possibilities to enhance properties where delocalization is important, such as in the case of transport. The demonstration of an order of magnitude boost in the mobility of organic semiconductors should be seen as a proof of principle, and further studies with optimized systems should lead to much higher enhancements. Another direction is to check physical phenomena that are sensitive to phonon energy. Metal–insulating and superconducting transitions for instance might be significantly modified under strong coupling.

It is already clear that chemical reactivity landscapes are very much altered by strong coupling. This also opens the possibility of achieving vibrational-state-selective chemistry at room temperature. Systematic studies of different classes of reactions under VSC need to be undertaken to extract general features induced by the hybridization. The effect of strong coupling on biological processes could also be investigated. The collective coupling implies that the molecules are quantum-mechanically indistinguishable, i.e., that events (charge recombination, emission, reactivity) will occur at the level of a molecule but that the particular molecule involved cannot be predicted. Coherent effects on (bio)chemical events might also be observed. The potential of strong coupling in spectroscopy and sensing, in homogeneous and heterogeneous catalysis, and in mechanistic studies has yet to be explored. Perhaps the most important drawback of strong coupling for such chemical applications is the fact that high concentrations are necessary to achieve significant Rabi splittings. It would thus be very important to find a way of amplifying the Rabi splitting. To better understand the properties of the hybrid states, further development of QED chemistry calculation methods, akin to those in quantum chemistry, would be extremely valuable.

Thus, light–matter hybridization offers many new opportunities for the molecular and materials sciences. It works in the absence of light, it is simple to implement, and its full potential is waiting to be explored.

AUTHOR INFORMATION

Corresponding Author

*E-mail: ebbesen@unistra.fr.

Notes

The author declares no competing financial interest.

Biography

Thomas W. Ebbesen is a physical chemist who was born in Oslo, Norway. He graduated from Oberlin College and then got his Ph.D. from P. & M. Curie University in Paris. He worked at the Notre Dame Radiation Laboratory, the NEC Fundamental Research Laboratories in Tsukuba, Japan, and the NEC Research Institute in Princeton before becoming a professor at the University of Strasbourg in 1999. He is currently the head of the Center for Frontier Research in Chemistry and the Strasbourg Institute for Advanced Studies (www.usias.fr). He holds the chair of physical chemistry of light–matter interactions. He is a member of the Norwegian Academy of Science and Letters and a foreign member of the French Academy of Science. Among other recognitions, he received the 2014 Kavli Prize in Nanoscience for his transformative contributions to nano-optics.

ACKNOWLEDGMENTS

The author is grateful for all the stimulating discussions on this subject with the members of the group during the past 10 years.

REFERENCES

- (1) Kasha, M. Energy Transfer Mechanisms and the Molecular Exciton Model for Molecular Aggregates. *Radiat. Res.* **1963**, *20*, 55–71.
- (2) Haroche, S.; Kleppner, D. Cavity Quantum Electrodynamics. *Phys. Today* **1989**, *42*, 24–30.
- (3) Kasprzak, J.; et al. Bose–Einstein Condensation of Exciton Polaritons. *Nature* **2006**, *443*, 409–414.
- (4) Skolnick, M. S.; Fisher, T. A.; Whittaker, D. M. Strong Coupling Phenomena in Quantum Microcavity Structures. *Semicond. Sci. Technol.* **1998**, *13*, 645–669.

- (5) Raimond, J. M.; Brune, M.; Haroche, S. Manipulating Quantum Entanglement with Atoms and Photons in a Cavity. *Rev. Mod. Phys.* **2001**, *73*, 565–582.
- (6) Agranovich, V. M.; Malshukov, A. G. Surface Polariton Spectra if the Resonance with the Transition Layer Exist. *Opt. Commun.* **1974**, *11*, 169–171.
- (7) Yakovlev, V. A.; Nazin, V. G.; Zhizhin, G. N. The Surface Polariton Splitting due to Thin Surface Film LO Vibrations. *Opt. Commun.* **1975**, *15*, 293–295.
- (8) Pockrand, I.; Brillante, A.; Möbius, D. Exciton–Surface Plasmon Coupling: An Experimental Investigation. *J. Chem. Phys.* **1982**, *77*, 6289–6295.
- (9) Fujita, T.; Sato, Y.; Kuitani, T.; Ishihara, T. Tunable Polariton Absorption of Distributed Feedback Microcavities at Room Temperature. *Phys. Rev. B: Condens. Matter Mater. Phys.* **1998**, *57*, 12428–12434.
- (10) Lidzey, D. G.; Bradley, D. D. C.; Skolnick, M. S.; Virgili, T.; Walker, S.; Whittaker, D. M. Strong Exciton–Photon Coupling in an Organic Semiconductor Microcavity. *Nature* **1998**, *395*, 53–55.
- (11) Kéna-Cohen, S.; Forrest, S. R. Room-temperature Polariton Lasing in an Organic Single-crystal Microcavity. *Nat. Photonics* **2010**, *4*, 371–375.
- (12) Plumhof, J. D.; Stöferle, T.; Mai, L.; Scherf, U.; Mahrt, R. F. Room-temperature Bose–Einstein Condensation of Cavity Exciton–Polaritons in a Polymer. *Nat. Mater.* **2014**, *13*, 247–252.
- (13) Daskalakis, K. S.; Maier, S. A.; Murray, R.; Kéna-Cohen, S. Nonlinear Interactions in an Organic Polariton Condensate. *Nat. Mater.* **2014**, *13*, 271–278.
- (14) Dintinger, J.; Klein, S.; Bustos, F.; Barnes, W. L.; Ebbesen, T. W. Strong Coupling between Surface Plasmon-Polaritons and Organic Molecules in Subwavelength Hole Arrays. *Phys. Rev. B: Condens. Matter Mater. Phys.* **2005**, *71*, 035424.
- (15) Schwartz, T.; Hutchison, J. A.; Genet, C.; Ebbesen, T. W. Reversible Switching of Ultrastrong Light–Molecule Coupling. *Phys. Rev. Lett.* **2011**, *106*, 196405.
- (16) Hutchison, J. A.; Schwartz, T.; Genet, C.; Devaux, E.; Ebbesen, T. W. Modifying Chemical Landscapes by Coupling to Vacuum Fields. *Angew. Chem., Int. Ed.* **2012**, *51*, 1592–1596.
- (17) Hutchison, J. A.; Liscio, A.; Schwartz, T.; Canaguier-Durand, A.; Genet, C.; Palermo, V.; Samori, P.; Ebbesen, T. W. Tuning the Work-Function via Strong Coupling. *Adv. Mater.* **2013**, *25*, 2481–2485.
- (18) Salomon, A.; Wang, S.; Hutchison, J. A.; Genet, C.; Ebbesen, T. W. Strong light–molecule coupling on plasmonic arrays of different symmetry. *ChemPhysChem* **2013**, *14*, 1882–1886.
- (19) Wang, S.; Mika, A.; Hutchison, J. A.; Genet, C.; Jouaiti, A.; Hosseini, M. W.; Ebbesen, T. W. Phase Transition of a Perovskite Strongly Coupled to the Vacuum Field. *Nanoscale* **2014**, *6*, 7243–7248.
- (20) Wang, S.; Chervy, T.; George, J.; Hutchison, J. A.; Genet, C.; Ebbesen, T. W. Quantum Yield of Polariton Emission from Hybrid Light-Matter States. *J. Phys. Chem. Lett.* **2014**, *5*, 1433–1439.
- (21) Canaguier-Durand, A.; et al. Thermodynamics of Molecules Strongly Coupled to the Vacuum Field. *Angew. Chem., Int. Ed.* **2013**, *52*, 10533–10536.
- (22) Canaguier-Durand, A.; Genet, C.; Lambrecht, A.; Ebbesen, T. W.; Reynaud, S. Non-Markovian Polariton Dynamics in Organic Strong Coupling. *Eur. Phys. J. D* **2015**, *69*, 24.
- (23) Shalabney, A.; George, J.; Hutchison, J. A.; Pupillo, G.; Genet, C.; Ebbesen, T. W. Coherent Coupling of Molecular Resonators with a Microcavity Mode. arXiv:1403.1050 [quant-ph] March 2014; idem. *Nat. Commun.* **2015**, *6*, 5981.
- (24) George, J.; Wang, S.; Chervy, T.; Canaguier-Durand, A.; Schaeffer, G.; Lehn, J.-M.; Hutchison, J. A.; Genet, C.; Ebbesen, T. W. Ultra-strong Coupling of Molecular Materials: Spectroscopy and Dynamics. *Faraday Discuss.* **2015**, *178*, 281–294.
- (25) Shalabney, A.; George, J.; Hiura, H.; Hutchison, J. A.; Genet, C.; Hellwig, P.; Ebbesen, T. W. Enhanced Raman Scattering from Vibro-Polariton Hybrid States. *Angew. Chem., Int. Ed.* **2015**, *54*, 7971–7975.
- (26) George, J.; Shalabney, A.; Hutchison, J. A.; Genet, C.; Ebbesen, T. W. Liquid-Phase Vibrational Strong Coupling. *J. Phys. Chem. Lett.* **2015**, *6*, 1027–1031.
- (27) Schwartz, T.; Hutchison, J. A.; Leonard, J.; Genet, C.; Haacke, S.; Ebbesen, T. W. Polariton Dynamics under Strong Light-Molecule Coupling. *ChemPhysChem* **2013**, *14*, 125–131.
- (28) Orgiu, E.; et al. Conductivity in organic semiconductors hybridized with the vacuum field. *Nat. Mater.* **2015**, *14*, 1123–1130.
- (29) Zhong, X.; Chervy, T.; Wang, S.; George, J.; Thomas, A.; Hutchison, J. A.; Devaux, E.; Genet, C.; Ebbesen, T. W. Non-Radiative Energy Transfer Mediated by Hybrid Light-Matter States. *Angew. Chem., Int. Ed.* **2016**, *55*, 6202–6206.
- (30) Thomas, A.; et al. Ground-state chemical reactivity under vibrational strong coupling to the vacuum electromagnetic field. *Angew. Chem., Int. Ed.* **2016**, *55*, 11462.
- (31) Houdré, R.; Stanley, R. P.; Illegems, M. Vacuum-Field Rabi Splitting in the Presence of Inhomogeneous Broadening: Resolution of a Homogeneous Linewidth in an Inhomogeneously Broadened System. *Phys. Rev. A: At., Mol., Opt. Phys.* **1996**, *53*, 2711–2715.
- (32) Törmä, P.; Barnes, W. L. Strong Coupling between Surface Plasmons Polaritons and Emitters: a Review. *Rep. Prog. Phys.* **2015**, *78*, 013901.
- (33) Bellessa, J.; Bonnard, C.; Plenet, J. C.; Mugnier, J. Strong coupling between surface plasmons and excitons in an organic semiconductor. *Phys. Rev. Lett.* **2004**, *93*, 036404.
- (34) Aberra Guebrou, S.; Symonds, C.; Homeyer, E.; Plenet, J. C.; Gartstein, Y. N.; Agranovich, V. M.; Bellessa, J. Coherent Emission from a Disordered Organic Semiconductor Induced by Strong Coupling with Surface Plasmons. *Phys. Rev. Lett.* **2012**, *108*, 066401.
- (35) Shi, L.; Hakala, T. K.; Rekola, H. T.; Martikainen, J.-P.; Moerland, R. J.; Törmä, P. Spatial Coherence Properties of Organic Molecules Coupled to Plasmonic Surface Lattice Resonances in the Weak and Strong Coupling Regimes. *Phys. Rev. Lett.* **2014**, *112*, 153002.
- (36) Galego, J.; Garcia-Vidal, F. J.; Feist, J. Suppressing Photochemical Reactions with Quantized Light Fields. 2015, arXiv:1606.04684. arXiv.org e-Print archive. <http://arxiv.org/abs/1606.04684> (accessed June 22, 2016).
- (37) Hoffmann, R. How Chemistry and Physics Meet in the Solid State. *Angew. Chem., Int. Ed. Engl.* **1987**, *26*, 846–878.
- (38) Wang, H.; et al. The role of Rabi splitting tuning in the dynamics of strongly coupled J-aggregates and surface plasmon polaritons in nanohole arrays. *Nanoscale* **2016**, *8*, 13445–13453.
- (39) Vasa, P.; Wang, W.; Pomraenke, R.; Lammers, M.; Maiuri, M.; Manzoni, C.; Cerullo, G.; Lienau, C. Real-time observation of ultrafast Rabi oscillations between excitons and plasmons in metal nanostructures with J-aggregates. *Nat. Photonics* **2013**, *7*, 128–132.
- (40) Zengin, G.; Wersäll, M.; Nilsson, S.; Antosiewicz, T. J.; Käll, M.; Shegai, T. Realizing strong light–matter interactions between single-nanoparticle plasmons and molecular excitons at ambient conditions. *Phys. Rev. Lett.* **2015**, *114*, 157401.
- (41) Berrier, A.; Cools, R.; Arnold, C.; Offermans, P.; Crego-Calama, M.; Brongersma, S. H.; Gómez-Rivas, J. Active control of the strong coupling regime between porphyrin excitons and surface plasmon polaritons. *ACS Nano* **2011**, *5*, 6226–6232.
- (42) Li, J.; Ueno, K.; Uehara, H.; Guo, J.; Oshikiri, T.; Misawa, H. Dual strong couplings between TPPS J-aggregates and aluminum plasmonic states. *J. Phys. Chem. Lett.* **2016**, *7*, 2786–2791.
- (43) Tumkur, T. U.; Zhu, G.; Noginov, M. A. Strong coupling of surface plasmon polaritons and ensembles of dye molecules. *Opt. Express* **2016**, *24*, 3921.
- (44) Melnikau, D.; et al. Rabi splitting in photoluminescence spectra of hybrid systems of gold nanorods and J-aggregates. *J. Phys. Chem. Lett.* **2016**, *7*, 354–362.
- (45) Carmeli, I.; Cohen, M.; Heifler, O.; Lilach, Y.; Zalevsky, Z.; Mujica, V.; Richter, S. Spatial modulation of light transmission through a single microcavity by coupling of photosynthetic complex excitations to surface plasmons. *Nat. Commun.* **2015**, *6*, 7334.

- (46) Ballarini, D.; et al. Polariton - induced enhanced emission from an organic dye under the strong coupling regime. *Adv. Opt. Mater.* **2014**, *2*, 1076–1081.
- (47) Ćwik, J. A.; Kirton, P.; De Liberato, S.; Keeling, J. Excitonic spectral features in strongly coupled organic polaritons. *Phys. Rev. A: At., Mol., Opt. Phys.* **2016**, *93*, 033840.
- (48) Herrera, F.; Spano, F. C. Cavity-controlled chemistry in molecular ensembles. *Phys. Rev. Lett.* **2016**, *116*, 238301.
- (49) Pellegrini, C.; Flick, J.; Tokatly, I. V.; Appel, H.; Rubio, A. Optimized effective potential for quantum electrodynamical time-dependent density functional theory. *Phys. Rev. Lett.* **2015**, *115*, 093001.
- (50) Zeng, P.; et al. Photoinduced Electron Transfer in the Strong Coupling Regime: Waveguide–Plasmon Polaritons. *Nano Lett.* **2016**, *16*, 2651–2656.
- (51) Cirio, M.; De Liberato, S.; Lambert, N.; Nori, F. Ground State Electroluminescence. *Phys. Rev. Lett.* **2016**, *116*, 113601.
- (52) Simpkins, B. S.; Fears, K. P.; Dressick, W. J.; Spann, B. T.; Dunkelberger, A. D.; Owrutsky, J. C. Spanning Strong to Weak Normal Mode Coupling between Vibrational and Fabry-Pérot Cavity Modes through Tuning of Vibrational Absorption Strength. *ACS Photonics* **2015**, *2*, 1460–1467.
- (53) Saurabh, P.; Mukamel, S. Two-dimensional infrared spectroscopy of vibrational polaritons of molecules in an optical cavity. *J. Chem. Phys.* **2016**, *144*, 124115.
- (54) Chikkaraddy, R.; et al. Single-molecule strong coupling at room temperature in plasmonic nanocavities. *Nature* **2016**, *535*, 127–130.
- (55) Feist, J.; Garcia-Vidal, F. J. Extraordinary exciton conductance induced by strong coupling. *Phys. Rev. Lett.* **2015**, *114*, 196402.
- (56) Schachenmayer, J.; Genes, C.; Tignone, E.; Pupillo, G. Cavity-Enhanced Transport of Excitons. *Phys. Rev. Lett.* **2015**, *114*, 196403.
- (57) Coles, D. M.; Somaschi, N.; Michetti, P.; Clark, C.; Lagoudakis, P. G.; Savvidis, P. G.; Lidzey, D. G. Polariton-Mediated Energy Transfer between Organic Dyes in a Strongly Coupled Optical Microcavity. *Nat. Mater.* **2014**, *13*, 712–719.
- (58) Cirio, M.; De Liberato, S.; Lambert, N.; Nori, F. Ground State Electroluminescence. *Phys. Rev. Lett.* **2016**, *116*, 113601.

■ NOTE ADDED AFTER ASAP PUBLICATION

This paper was published ASAP on October 25, 2016, with an error to Figure 4 and Figure 5. The corrected version was reposted on October 28, 2016.